Available online at www.sciencedirect.com

ScienceDirect

Materials Today: Proceedings 5 (2018) 27526–27535

materialstoday: PROCEEDINGS

www.materialstoday.com/proceedings

PSCCE_2017

Effects of the filler's loading in features of poly(acrylic acid)/graphene oxide nanocomposites

K. Karatasos* and G. Kritikos

Chemical Engineering Department, Aristotle University of Thessaloniki, Thessaloniki 54124, Greece

Abstract

Poly(acrylic acid)(PAA)/Graphene oxide(GO) nanocomposites of two different loadings in GO were examined using molecular dynamics simulations. It was found that increasing of the GO loading imparted a progressively higher degree of slowing down of local dynamics, particularly near the PAA/GO interface. As the GO content increased the intermolecular PAA hydrogen bonding decreased, but neither the PAA intramolecular nor the PAA/GO hydrogen bond formation was affected. Global chain dynamics became slower as the GO concentration increased due to the effective confinement of the polymer chains. Increase of the GO loading affected the temperature dependence of both, local and global polymer dynamics.

Selection and/or Peer-review under responsibility of 11th Panhellenic Scientific Conference on Chemical Engineering.

Keywords: Graphene oxide; Poly(acrylic acid); Nanocomposites; Molecular dynamics simulations; Hydrogen bonding; Polymer dynamics;

1. Introduction

Optimization of the properties of polymer-based composite materials is among the main targets of current industrial and scientific research [1]. Towards this direction, computer simulations have proven a valuable tool which can provide detailed information, usually not accessible to available experimental techniques, regarding the elementary mechanisms which operate at the molecular/atomic level and essentially dictate the macroscopic properties of the examined materials [2]. Such elementary mechanisms, related for instance to the polymer physical adsorption on the filler's surface [3] and the changes in chain conformations and polymer dynamics close to the polymer/filler interface [4, 5], may affect drastically the observed physical behavior of these composites. Therefore,

* Corresponding author. Tel.: +302310995850; fax: +302310996222.
E-mail address: karatas@eng.auth.gr

Selection and/or Peer-review under responsibility of 11th Panhellenic Scientific Conference on Chemical Engineering.

elucidation of the details on the processes that take place at the microscopic level may lead to the desired property optimization of the composite systems.

One of the categories of polymer composite materials that have recently attracted a strong academic and technological interest are those comprised by graphene-based fillers [6, 7], due to the exceptional properties of graphene, which when combined with those of the polymeric matrix may lead to the fabrication of high added value products. In our case we examine systems comprised by graphene oxide (GO) and poly(acrylic acid) (PAA). Such systems can be considered as candidates for energy related applications, e.g., as solid polyelectrolyte membranes used in batteries and fuel cells [8, 9]. The present work is an extension of our previous study on PAA/GO nanocomposites [10], focusing on the effects of the increase in the filler's content on the morphological characteristics of the polymer chains, the hydrogen -bonding pattern between PAA chains and between PAA and GO, as well as on local and global polymer dynamics.

2. Description of the systems and the simulation details

2.1. Description of the examined systems

The model used for the GO flakes, together with the monomer of PAA are shown schematically in figure 1.

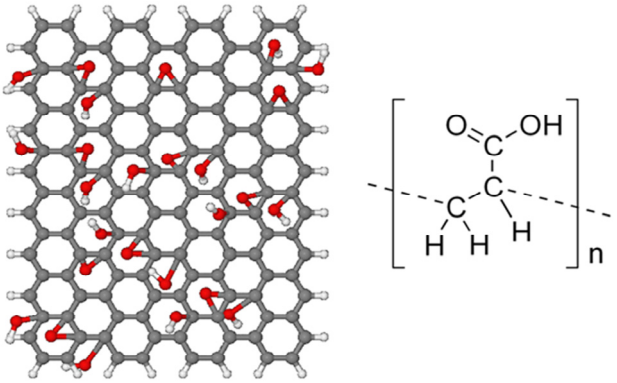

Fig. 1. Structure of the GO flake (left) and the PAA monomer (right)

The lateral dimensions of each GO flake were 15 Å x 20 Å which were comparable to the average size of each PAA chain (estimated to be about 14 Å). The structure of the graphene-oxide flake follows that of ref. [11] bearing a carbon to oxygen atom ratio of 5:1 and a hydroxyl to epoxy group ratio of 3:2 approximately, while is terminated with hydrogen atoms. Each polymeric chain was comprised by 40 monomers arranged in an atactic manner. The notation and the characteristics of the systems that are compared in the present study are listed in Table 1.

Table 1. Description of the systems compared in this work

System Notation	Number of GO sheets	Number of PAA chains	wt % in GO
40paa40	0	40	0.0
30paa7GO	7	30	14.5
30paa18GO	18	30	30.3

2.2. Simulation details

The energetic parameters for the description of both the components were based on the AMBER forcefield [12] and the partial charges of each atom were obtained as is described in more detail in our previous work [10]. The

systems were simulated using the isothermal isobaric statistical ensemble (NPT) with a timestep of 1 fs, a frame saving frequency of 1 ps and a pressure of 1 bar, under periodic boundary conditions, using the NAMD package [13]. Each system has undergone a thermal annealing procedure from 300K up to 650K every 50K for equilibration purposes, followed by a cooling process starting from 650K down to 300K with the same temperature step. All analysis was performed in the production runs, amounting to several hundred ns, obtained from the cooling part. The interested reader may refer to ref. [10] for more details regarding the simulation protocol followed. Figure 2 depicts the starting configuration and the equilibrated structures obtained in the cooling part, at T=400K and T=500K.

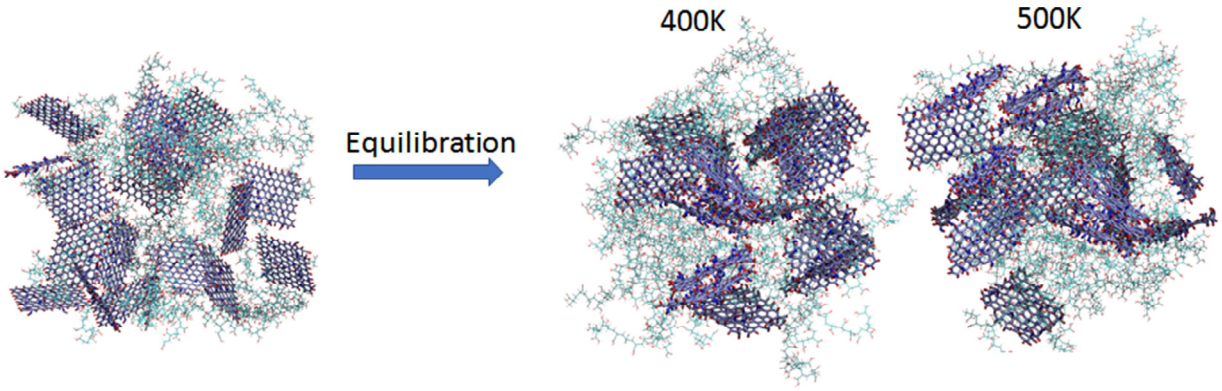

Fig. 2. Snapshots of the 30paa18GO systems immediately after the construction (left) and after the equilibration procedure, at two temperatures

As can readily be observed from the equilibrated snapshots, graphene oxide forms clusters mainly comprised by 2-3 flakes in line with previous simulation and experimental results in graphene-based polymer composites [14, 15]. In addition, it must be noted that the geometry of the GO flakes departs from that of a perfectly planar shape. Therefore, the definition of a GO plane was based on the two principal axes of inertia of the flake which were on average parallel to the GO surface. The direction of the third axis which completed the orthogonal system of the principal axes of inertia, defined the direction of the GO plane.

3. Results and discussion

3.1. Effects of GO concentration on chain shape in the composites

As was noted in our previous work were comparison was made between the average shape of PAA chains in the pristine polymer and in the 30paa7GO system, [10] the presence of GO did not appear to affect appreciably the average shape parameters of the polymer chains. Increase of the GO concentration to almost double an amount (i.e. from 14.5 wt% in 30paa7GO to 30.3 wt% in 30paa18GO) left the chain shape characteristics practically unaltered as well, as this is portrayed in figure 3. To check the picture characterizing the behavior of the chains close to the PAA/GO interface we have calculated the average dimensions of the ellipsoid of inertia, as a function of the distance of the center of mass of a chain from a GO plane. Figure 4 shows the behavior of the longest axes of the ellipsoid of inertia at the examined temperatures.

Evidently, as the temperature drops, the chains close to the GO plane tend to assume more elongated conformations. This trend is more prominent in the system with a higher GO loading. This could be related to the fact that the percentage of chains close to a GO surface is higher in the 30paa18GO system, while, in addition, the chains in this system essentially experience a higher degree of confinement due to the higher GO loading. The degree of chain shape deformation along the two other axes of the ellipsoid of inertia close to the GO surface (not shown here), is considerably smaller. The observed degree of PAA shape deformation close to the GO surface, appears to be lower compared to the behavior observed in previous graphene-based polymer nanocomposites [16].

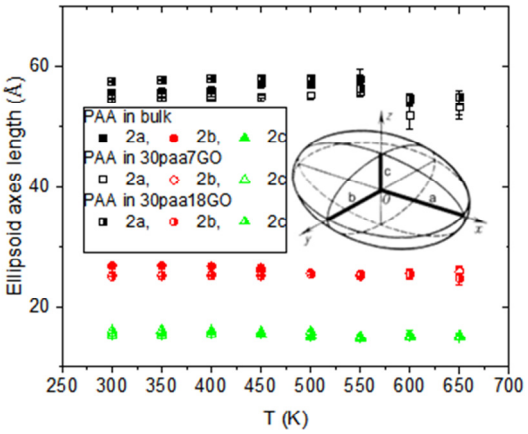

Fig. 3. Axes of the ellipsoid of inertia of the polymer chains in the pristine PAA model (filled symbols) and in the nanocomposites (open and semi-filled symbols) at the examined temperature range.

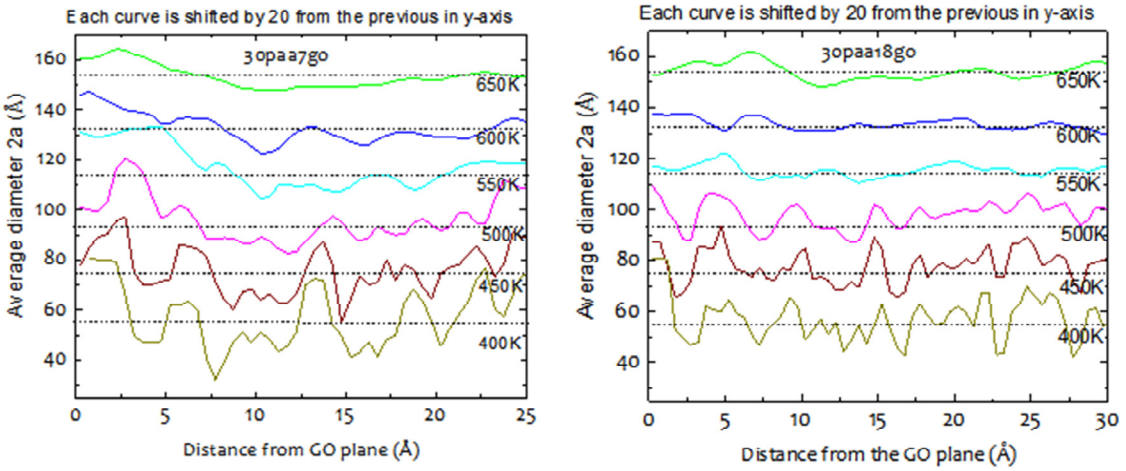

Fig. 4. The longest axis of the ellipsoid of inertia of the polymer chains in the two composites, at different temperatures.

Apart from differences that can be related to the strength of the interactions between the polymer matrix and the graphene-based filler, this can be also attributed to the fact that in our case the GO platelets are not perfectly planar (see fig.2), disfavoring thus a much denser packing of the chains close to the GO surface.

3.2. Effects of GO concentration on the degree of hydrogen bonding

The role of specific interactions between the polymer and the filler in composite materials, is crucial when it comes to the morphology of the resulted dispersion and the characteristics of the physical adsorption of the chains onto the filler's surface [17, 18]. Since both of the components in the examined systems bear hydrogen-bonding-capable donor-acceptor pairs, we have examined the degree of hydrogen bonding between the PAA chains (of intra- and intermolecular nature) as well as those between polymer chains and GO. The determination of hydrogen-bonded pairs was performed based on geometric criteria, as described in ref[10]. Figure 5 illustrates the degree of hydrogen bonding between the hydroxyl hydrogens (HO) and hydroxyl oxygens (OH) belonging to the PAA chains.

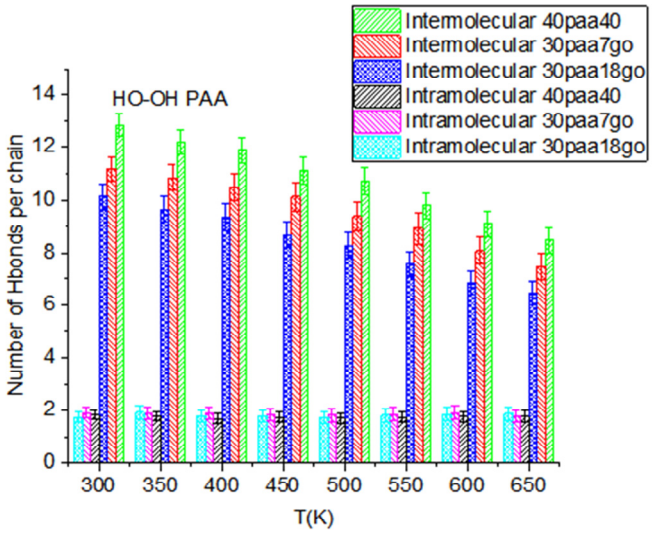

Fig. 5. Average number of intra- and intermolecular HO-OH hydrogen bonds per chain, in the pristine system and in the nanocomposites

In all models the number of the examined intermolecular hydrogen bonds increases as temperature drops due to the densification of the systems but that describing intramolecular hydrogen bonding remains independent of temperature. In the nanocomposites the presence of GO reduces on average the degree of intermolecular hydrogen bonding, since GO intervenes between the polymer chains obstructing thus partly the interchain hydrogen bond formation. This interpretation is consistent with the lower degree of the interchain hydrogen-bonding as concentration of GO increases. The degree of intrachain hydrogen bonding however, appears to be insensitive to the presence of GO.

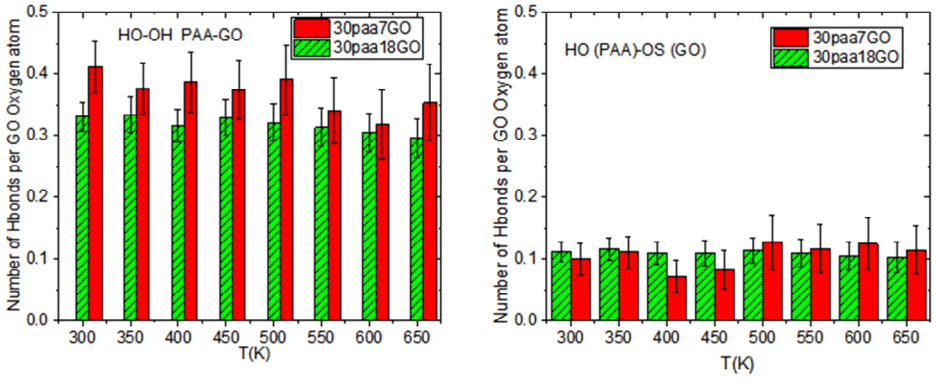

Fig. 6. Average number of PAA/GO hydrogen bonds per GO oxygen atom between the hydroxyl oxygen (OH) – hydroxyl hydrogen (HO) (left) and the PAA hydroxyl hydrogen (HO) – GO epoxy oxygen (OS) (right).

As was noted in our previous work [10], hydrogen bonding between PAA and GO is dominated by the HO-OH pairs. Actually, it appears that the increase in GO content has only a minor effect on the PAA/GO hydrogen bonding as shown in figure 6. The same insensitivity on GO content is also observed when examining the hydrogen bonding dynamics (not shown here) as the GO content increases (see also ref. [10]). Due to its local nature, dynamics of formation and disruption of hydrogen bonds is not practically affected by the increased GO loading, at least within the examined range of GO concentrations.

3.3. Effects of GO concentration on chain dynamics

For the examination of the overall chain reorientational motion we have computed the 2nd order correlation function of unit vectors $\hat{k}(t)$ connecting the center of mass of a polymer chain with its atoms, according to eq 1

$$C_2(t) = \frac{1}{2}\left\langle 3\left[\hat{k}(t)\cdot\hat{k}(0)\right]^2 - 1\right\rangle \quad (1)$$

Angle brackets denote time and ensemble average over all vectors per chain and over all chains. Figure 7 compares such correlation functions of PAA chains in the examined systems.

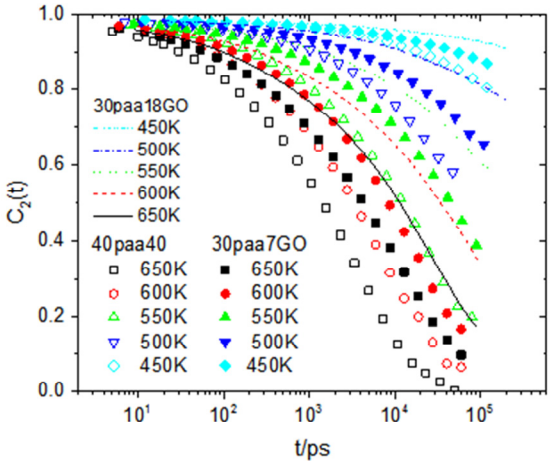

Fig. 7. Overall reorientational correlation functions for PAA chains in the examined systems.

Visual inspection of the computed chain reorientational spectra indicates that the degree of decorrelation decreases (i.e., the timescale for the complete decorrelation shifts to longer times) as the GO loading increases. This is a direct evidence that PAA chains in the composites experience a much more constricted environment in comparison to the pristine system, which results in the retardation of the chain rotational diffusion. To quantify the degree of slowing down at the chain rotational motion, we have estimated characteristic relaxation times (even at lower temperatures at which complete decorrelation of the dynamic spectra is not accomplished within the simulation window), by performing a time-temperature shifting procedure. According to this procedure, we take one temperature as reference and then shift the rest of the curves in order to form a mastercurve. In this manner, if this procedure is successful, we can calculate the shift factor for the examined temperatures. Then by calculating the relaxation time for a curve that decorrelates sufficiently within the simulation window and by using these shift factors we can estimate the relaxation times for the remaining temperatures as well. Application of this procedure is presented as an example in figure 8 for the 30paa18GO model. As shown, all curves appearing in figure 7 for the 30paa18GO system, successfully superpose onto a single mastercurve. The results of the shifting procedure for the pristine system and the 30paa7GO composite (see the supporting material in ref. [10]) are very similar.

As was implied from the behavior described in figure 7, the relaxation rates in the composites are lower compared to those in the pristine PAA. Actually, the higher the loading of GO the slower the overall chain dynamics, indicating the effect of the increasingly more confined microenvironment experienced by the polymer chains as the matrix becomes more populated in GO. It is also noteworthy that the temperature dependence of the relaxation rates changes as the GO content increases. The rates describing the lower in GO loading sample follow a temperature dependence very similar to that of the pristine polymer, while the degree of slowing down amounts to a factor close to 2. The rates corresponding to the chain relaxation in the sample with the higher GO concentration appear to follow a different temperature dependence, while the degree of slowing down in considerable larger, amounting to a factor of 10 or higher as the temperature drops. The apparently stronger temperature dependence in the 30paa18GO model is consistent with a relaxation mechanism more cooperative in nature, which can be

rationalized by the more constricted environment accompanied by a higher probability of a chain to be located close to a GO surface

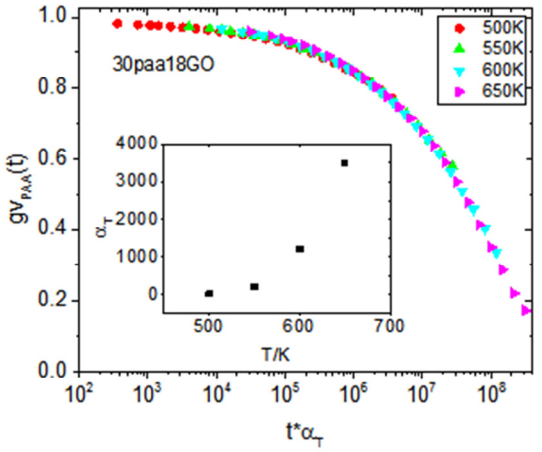

Fig. 8. Result of the shifting procedure as described in the text for the 30paa18GO system. Inset presents the temperature dependence of the shift factors.

Figure 9 compares the estimated average relaxation rates for the overall chain rotation in all the examined systems.

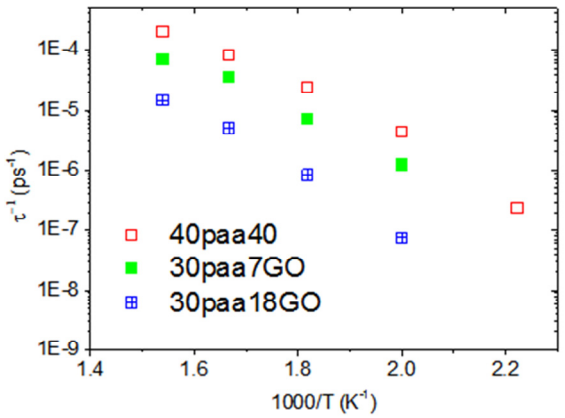

Fig. 9. Chain rotational relaxation rates (see text) as a function of temperature in the pristine polymer and in the composites

3.4. Effects of GO concentration on local dynamics

Local polymer dynamics were probed by computing rotational correlation functions $g_2(t)$ of backbone C-C bonds. The expression defining $g_2(t)$ is analogous to that in eq 1, with $\hat{k}(t)$ representing now unit vectors along the examined bonds. Fourier transform of the $g_2(t)$ functions lead to the calculation of the spectral density which is closely related to Neutron Magnetic Resonance (NMR) measurements [19].

As it was demonstrated in our previous work [10] the presence of GO in system 30paa7GO was found to slow down the average bond reorientational motion with respect to that of the pristine PAA model. In addition, it was found that the higher contribution to the average slowing down was originating from those bonds located close to the PAA/GO interface. To check whether the increase of GO concentration will affect this behavior, we have calculated the $g_2(t)$ correlation functions arising from the overall average of the bonds, as well as those that take into account only bonds that belong to the first layer close to the GO surface. The width of the layer is taken to be 5Å, as this is defined by the first peak in the polymer density profile along a direction normal to the GO plane (not shown here for the system 30paa18GO, but analogous to that described in ref. [10]). Figure 10 compares $g_2(t)$ spectra arising from all C-C backbone bonds in the two composite systems, and their analogues describing the overall average and the dynamics in the 1st layer in the 30paa18GO system.

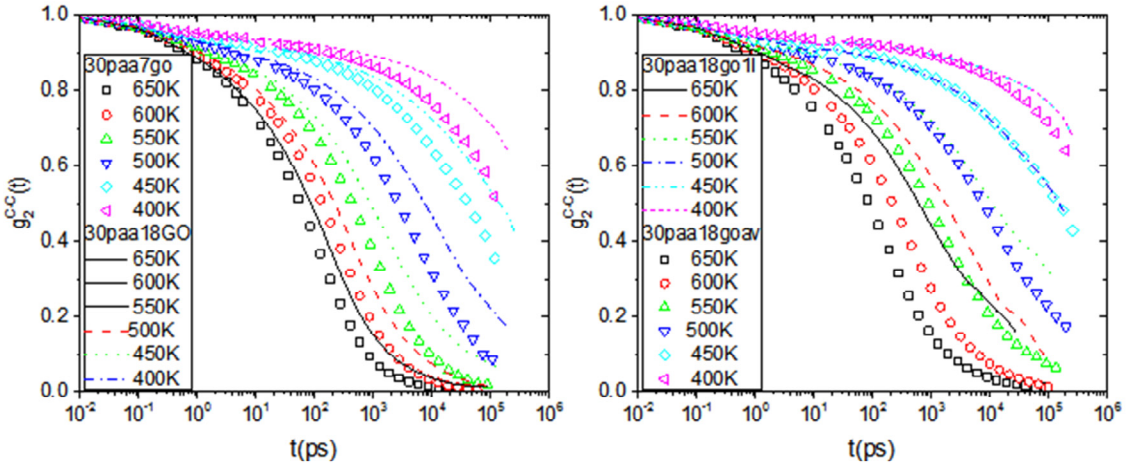

Fig. 10. Comparison of the overall average bond reorientational correlation functions of PAA chains in the two nanocomposites (left) and those of the overall average and of the 1st layer close to the GO surface, for the 30paa18GO system (right).

As was shown for the 30PAA7GO system [10], correlation functions characterizing bond dynamics in the 1st layer, decay at a lower degree with respect to those describing the corresponding temperatures of the overall average bond motion in the 30PAA18GO model, as well (fig. 10, right). The effect of the GO concentration in bond dynamics is demonstrated when comparing the average behavior in the two composites (fig. 10, left). It appears that the decorrelation of functions in the highly populated system in GO takes place at longer timescales. This effect can be rationalized if we take into account that at the 30PAA18GO system the percentage of bonds close to the GO surface is higher.

To map the observed differences in the bond reorientation timescales, we have plotted the relaxation rates corresponding to the time it takes for the PAA C-C bond correlation functions to drop to the 1/e of their initial values [10]. Figure 11 describes the overall average bond dynamics in the 3 systems and the bond motion in the 1st polymer layer close to the GO plane in the two composites.

A visual comparison of the PAA C-C bond relaxation rates at the first layer in the composite systems, shows that apart from their lower values they also assume a stronger temperature dependence when compared to the average bond behavior. Moreover, the interfacial bonds in the 30paa18GO system relax at lower rates with respect to those in the 30PAA7GO system. Since the strength of GO/PAA interactions are essentially similar in the two composites due to the insensitivity of the PAA/GO hydrogen-bond population in the GO loading (see fig. 6), an additional mechanism should be present which can give rise to the observed differences in the interfacial bond dynamics between the two composites. Such a mechanism can be envisaged if we bear in mind that longer lengthscale modes may affect dynamics at local scale (i.e. that of the bond or that of the statistical segment) [20, 21] and recall that the overall chain rotational motion becomes slower as the GO loading increases (fig. 9). In addition, the degree of

dynamic heterogeneity in the local microenvironment might differ in the two composites due to differences in the local density distributions, caused by distinct GO dispersion characteristics in the two composites.

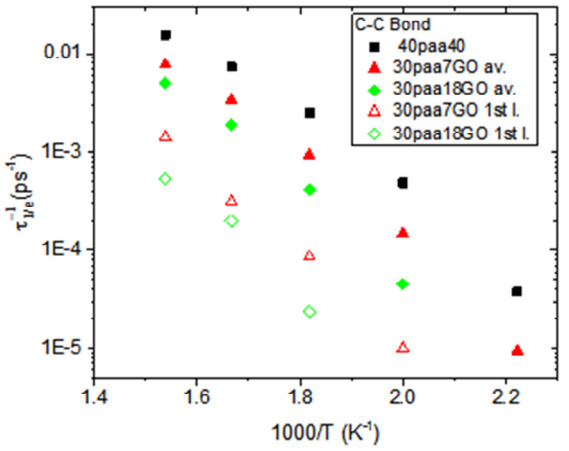

Fig. 11. Relaxation rates (see text) of PAA C-C bond reorientational motion for the overall average (filled symbols) and for the 1st layer adjacent to the GO surface (open symbols), as a function of temperature.

The larger slowing down of local motion in the composite with the higher GO content, implies a slower polymer α-relaxation, which in turn implies a higher glass transition temperature in the 30paa18GO composite. An estimation of the glass transition temperature in the latter system based on a modified Sanchez – Lacombe equation of state [22] following the procedure described in ref. [10], rendered a value of approximately 530K, about 80K higher compared to the value of 450K estimated for the 30paa7GO composite [10]. This issue will be discussed in more detail in a forthcoming publication.

4. Conclusions

Poly(acrylic acid)(PAA)/Graphene oxide(GO) nanocomposites of two different loadings in GO were examined in a wide temperature range by means of fully atomistic molecular dynamics simulations, in order to assess the effects of the filler's content on the morphological characteristics of the polymer chains, the hydrogen-bonding pattern between PAA molecules and between PAA and GO, as well as on local and global polymer dynamics. An noticeable degree of slowing down of backbone bond dynamics was observed as the GO content was augmented, which was enhanced close to the PAA/GO interface. This effect can be correlated with the shift of the glass transition to higher temperatures in the composites, as the GO loading increased. The observed slowing down was accompanied by a stronger temperature dependence of bond relaxation times with respect to that describing the pristine PAA, upon increase of the GO loading. The degree of hydrogen bond formation between PAA and GO, driven mainly by the hydroxyl hydrogens and the hydroxyl oxygens pairs present in the two molecular moieties, was found to be insensitive to the GO loading. Polymer chains close to the GO surface assumed more elongated conformations compared to those afar from the interface, with this effect being more enhanced in the high GO content system. Average dynamics in the global polymer scale became slower in the composite systems, while a stronger temperature dependence was noticed in the system with the higher GO concentration. The slowing down in global and local polymer motion and the observed changes in the temperature dependence of the respective relaxation times can be rationalized on accounts of the effective constriction experienced by the polymer chains upon increase of the graphene oxide loading and the polymer physical adsorption onto the GO

surface respectively, in conjunction with changes in the local microenvironment (i.e. in density/free volume distribution) triggered by the different characteristics of the GO dispersion when its concentration varies.

References

[1] L.I. Bazylak, G.E. Zaikov, A.K. Haghi, Polymers and Polymeric Composites - Properties, Optimization, and Applications Apple Academic Press, New Jersey, 2015.
[2] S. Roy, J.N. Reddy, in: J.N. Reddy (Ed.) Computational Modeling of Polymer Composites, CRC Press, New York, 2014.
[3] P. Kelich, A. Asadinezhad, J Mol Graph Model, 69 (2016) 26-38.
[4] A.N. Rissanou, V. Harmandaris, Soft Matter, 10 (2014) 2876-2888.
[5] R.-E. Roussou, K. Karatasos, Mater Design, 97 (2016) 163-174
[6] K. Karatasos, Macromolecules, 47 (2014) 8833-8845.
[7] P. Mukhopadhyay, R.K. Gupta, Graphite, Graphene, and their polymer nanocomposites, CRC Press, 2013.
[8] C.-W. Liew, H.M. Ng, A. Numan, S. Ramesh, Polymers, 8 (2016) 179.
[9] B. Smitha, S. Sridhar, A.A. Khan, Macromolecules, 37 (2004) 2233-2239.
[10] K. Karatasos, G. Kritikos, RSC Adv., 6 (2016) 109267.
[11] D. Stauffer, N. Dragneva, W.B. Floriano, R.C. Mawhinney, G. Fanchini, S. French, O. Rubel, J Chem Phys, 141 (2014) 044705.
[12] W.D. Cornell, P. Cieplak, C.I. Bayly, I.R. Gould, K.M. Merz, D.M. Ferguson, D.C. Spellmeyer, T. Fox, J.W. Caldwell, P.A. Kollman, J. Am. Chem. Soc., 117 (1995) 5179-5197.
[13] J. Phillips, R. Braun, W. Wang, J. Gumbart , E. Tajkhorshid, E. Villa, C. Chipot, R. Skeel, L. Kale, K. Schulten, J. Comput. Chem. , 26 (2005) 1781–1782.
[14] L. Gong, R.J. Young, I.A. Kinloch, I. Riaz, R. Jalil, K.S. Novoselov, ACS Nano, 6 (2012) 2086-2095.
[15] R.J. Young, I.A. Kinloch, L. Gong, K.S. Novoselov, Compos. Sci. Technol., 72 (2012) 1459-1476.
[16] A. Rissanou, V. Harmandaris, J Nanopart Res, 15 (2013) 1-14.
[17] D. Pramanik, P.K. Maiti, Soft Matter, 12 (2016) 8512-8520.
[18] I. Szleifer, R. Yerushalmi-Rozen, Polymer, 46 (2005) 7803-7818.
[19] K. Karatasos, J.P. Ryckaert, R. Ricciardi, F. Lauprêtre, Macromolecules, 35 (2002) 1451-1462.
[20] K. Karatasos, D.B. Adolf, J. Chem. Phys., 112 (2000) 8225-8228.
[21] H. Morhenn, S. Busch, H. Meyer, D. Richter, W. Petry, T. Unruh, Phys. Rev. Lett., 111 (2013).
[22] G. Kritikos, Polymer, 55 (2014) 4658-4670.